Evgeny Tsymbal Publications

Research Papers in Physics and Astronomy

Bias voltage dependence of tunneling anisotropic magnetoresistance in magnetic tunnel junctions with MgO and Al_2O_3 tunnel barriers

Li Gao
IBM Research Division, Almaden Research Center, San Jose, California

Xin Jiang
IBM Research Division, Almaden Research Center, San Jose, California

See-Hun Yang
IBM Research Division, Almaden Research Center, San Jose, California

John D. Burton
University of Nebraska-Lincoln, jburton2@unl.edu

Evgeny Y. Tsymbal
University of Nebraska at Lincoln, tsymbal@unl.edu

See next page for additional authors

Authors

Li Gao, Xin Jiang, See-Hun Yang, John D. Burton, Evgeny Y. Tsymbal, and Stuart S. P. Parkin

Bias Voltage Dependence of Tunneling Anisotropic Magnetoresistance in Magnetic Tunnel Junctions with MgO and Al$_2$O$_3$ Tunnel Barriers

Li Gao,[1,2] Xin Jiang,[1] See-Hun Yang,[1] J. D. Burton,[3] Evgeny Y. Tsymbal,[3] and Stuart S. P. Parkin[1]

[1]*IBM Research Division, Almaden Research Center, San Jose, California 95120, USA*
[2]*Department of Applied Physics, Stanford University, Stanford, California 94305, USA*
[3]*Department of Physics and Astronomy, University of Nebraska–Lincoln, Lincoln, Nebraska 68588, USA*
(Received 19 February 2007; revised manuscript received 2 July 2007; published 27 November 2007)

Tunneling anisotropic magnetoresistance (TAMR) is observed in tunnel junctions with transition metal electrodes as the moments are rotated from in-plane to out-of-plane in sufficiently large magnetic fields that the moments are nearly parallel to one another. A complex angular dependence of the tunneling resistance is found with twofold and fourfold components that vary strongly with bias voltage. Distinctly different TAMR behaviors are obtained for devices formed with highly textured crystalline MgO(001) and amorphous Al$_2$O$_3$ tunnel barriers. A tight-binding model shows that a fourfold angular dependence can be explained by the presence of an interface resonant state that affects the transmission of the contributing tunneling states through a spin-orbit interaction.

Magnetic tunnel junctions (MTJs) can exhibit very large changes in resistance when the relative alignment of the electrode moments is switched [1]. This tunneling magnetoresistance (TMR) is largely determined by the spin polarization of the tunneling current, which is a consequence, not simply of the spin-polarized density of states (DOS) of the ferromagnetic electrodes, but also of the tunneling matrix elements [2,3], and the spin-dependent decay of the electron wave functions across the tunnel barrier [4–6]. Using electrodes formed from the 3d transition metal (TM) ferromagnets, such as Co-Fe alloys, and tunnel barriers formed from Al$_2$O$_3$ and MgO, TMR values of up to ~70% and ~470% are observed at room temperature, respectively [5–8]. Of particular interest is the influence of the detailed electronic structure of the MTJ on the bias voltage dependence of the spin-polarized tunneling. One way to probe such an effect is to consider the *angular* dependence of the tunneling resistance, or the tunneling anisotropic magnetoresistance (TAMR) when the electrode's moments are rotated in large magnetic fields.

A large TAMR effect was recently observed in distinctly different MTJs formed from semiconductor heterostructures in which the ferromagnetic electrodes are formed from Mn doped GaAs [9–11]. Spin-orbit coupling (SOC) plays an important role in this material so that the TAMR effect could be attributed to a significant anisotropy in the DOS linked to the magnetization direction along different crystal axes [9–11]. Although SOC is much weaker in TMs, a small TAMR effect has been predicted for tunnel junctions with TM electrodes [12,13]. These calculations did not, however, consider the detailed bias or the angular dependence of the TAMR effect. In this Letter we show that MTJs with CoFe electrodes exhibit a TAMR effect, which, albeit small in magnitude, displays a complex angular dependence and has a strong dependence on the bias voltage and on the tunnel barrier material.

MTJs were fabricated on thermally oxidized Si substrates using a combination of ion-beam and magnetron sputtering at ambient temperature. A small in-plane magnetic field was applied during deposition to define the easy axis of the magnetic films. *In situ* shadow masks were used to pattern junctions ~80 × 80 μm^2 in area. After deposition, the devices were annealed at 260 °C for 30 minutes in a 1 T field. Two types of MTJs, with CoFe ferromagnetic electrodes and a MgO or Al$_2$O$_3$ tunnel barrier, were fabricated with the following structures (from bottom to top): 100 MgO/50 Ta/250 Ir$_{22}$Mn$_{78}$/3 Co$_{49}$Fe$_{21}$B$_{30}$/60 Co$_{70}$Fe$_{30}$/34 MgO/25 Co$_{70}$Fe$_{30}$/150 Co$_{49}$Fe$_{21}$B$_{30}$/100 Ta/ and 100 TaN/75 Ta/250 Ir$_{24}$Mn$_{76}$/5 Co$_{49}$Fe$_{21}$B$_{30}$/40 Co$_{70}$Fe$_{30}$/25 Al$_2$O$_3$/20 Co$_{70}$Fe$_{30}$/100 Co$_{49}$Fe$_{21}$B$_{30}$/50 Ta/ 75 Ru, where the numbers are nominal layer thicknesses in Å.

Magnetotransport measurements, both dc and ac, were carried out at 10 K in a low temperature cryostat equipped with a sample rotator and a superconducting magnet. An ac lock-in technique was used to measure the dynamic resistance $R_D = dV/dI$ of the tunnel junctions, with a modulation amplitude of 8 mV rms at 1001 Hz. A dc bias voltage was simultaneously applied during the dV/dI measurement, with positive bias corresponding to current flowing from bottom to top. The experiment geometry was such that the magnetic field $\vec{H}$, the normal to the film plane $\vec{n}$, and the magnetic easy axis were arranged in the same plane [Fig. 1(a)]. The field direction was fixed during the experiment and the sample was rotated so that the field direction was rotated from in-plane to out-of-plane. The dc and dynamic resistances were measured, using a four-point technique, as a function of the angle θ between $\vec{H}$ and $\vec{n}$. θ values of 0°, 180°, and 360° correspond to magnetic fields perpendicular to the film plane, while 90° and 270° correspond to fields along the in-plane easy axis direction.
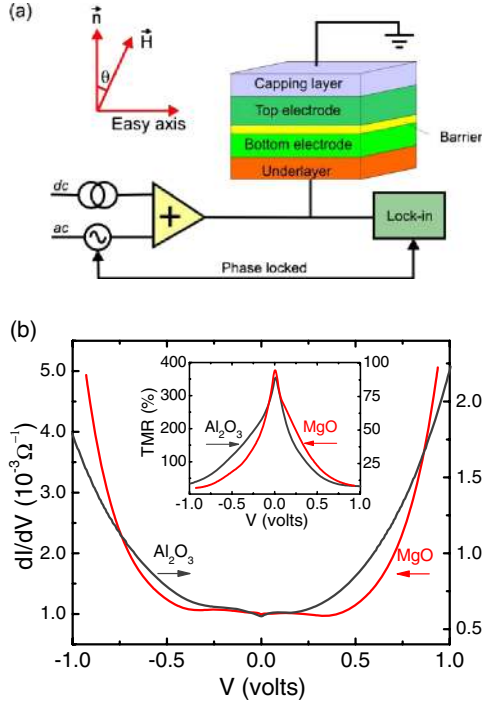
FIG. 1 (color online).   Schematic diagram of the TAMR measurement setup (a) and the bias dependence of differential conductance for the MgO and Al_2O_3 MTJs in a perpendicular field of 7 T at 10 K (b). The inset in (b) shows the bias dependence of the differential TMR at 10 K.

FIG. 2 (color online).   Normalized R_D vs θ curves (symbols) at various bias voltages for MgO (a) and Al_2O_3 (b) MTJs. The data are displaced vertically for clarity. The solid lines are fits using Eqs. (1) and (2). (c),(d) The fitting parameters A_2/A_0 (solid circles) and A_4/A_0 (open squares) as a function of bias for the MgO and Al_2O_3 MTJs.

Figure 1(b) depicts the differential conductance dI/dV as a function of bias voltage at 10 K in a perpendicular field of 7 T ($\theta = 0°$), for MTJs with Al_2O_3 and MgO tunnel barriers, respectively. Data at $\theta = 90°$ closely resemble those at $\theta = 0°$. The inset in Fig. 1(b) shows the corresponding bias dependence of the differential TMR, defined as $[(dI/dV)_P - (dI/dV)_{AP}]/(dI/dV)_{AP}$. Here dI/dV is measured in an in-plane field; P and AP stand for parallel and antiparallel alignment of the CoFe moments, respectively. Zero-bias TMR values of 377% and 89% were obtained for the MTJs with MgO and Al_2O_3 barriers, respectively, indicating the high quality of these devices.

R_D vs θ curves at various bias voltages are plotted in Fig. 2(a) for the MgO junction. The measurements were taken at 10 K in a field of 7 T, which is sufficiently large to almost fully saturate the magnetization of the CoFe electrodes parallel to the field. The junction resistance is normalized to its average value over θ at each bias voltage. At low bias, the R_D vs θ curves are twofold symmetric, with peaks at $\theta = 0°$, $180°$, $360°$, and valleys at $\theta = 90°$, $270°$. As the bias is increased, the valleys near $\theta = 90°$, $270°$ broaden and, eventually, a second set of peaks appears for bias voltages exceeding ~ -0.4 V or $+0.45$ V. This suggests that an additional component with fourfold symmetry contributes to TAMR at high bias. The magnitude of TAMR is fairly symmetric with respect to bias polarity at low bias. At high bias, however, TAMR is much smaller for positive bias.
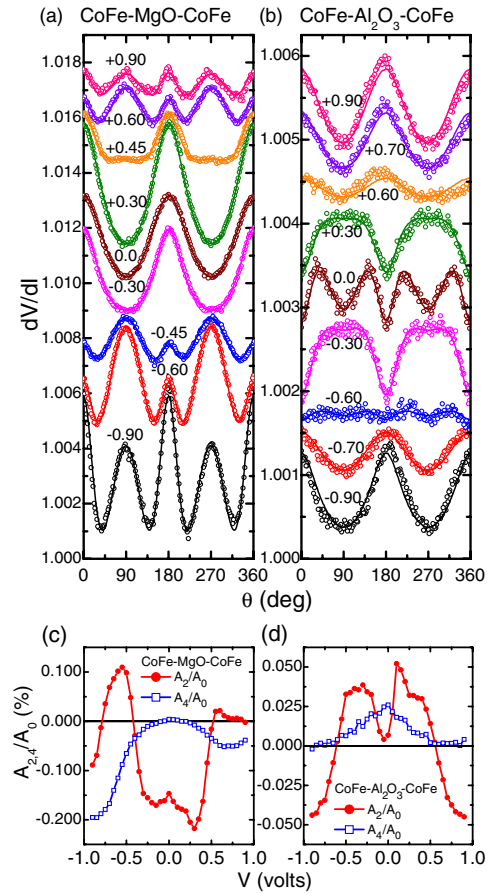
In Figs. 3(a) and 3(c), the normalized junction resistance is plotted as a function of bias and angle, for the dynamic and dc resistance measurements, respectively. The data were taken, in each case, every 2° and every 50 mV (note that in the dc case no data are possible at zero bias). The contrast in the contour plot represents the magnitude of the normalized junction resistance. The dc and dynamic resistances measure different quantities. The former integrates contributions from electrons distributed over a wide energy range up to the bias voltage, whereas the latter is sensitive to tunneling in a narrow energy range, determined by the modulation amplitude (here, ~ 24 mV, peak to peak). The ac measurement clearly accentuates the dependence of the TAMR effect on both voltage and angle, as shown in Fig. 3. For this reason, we focus our discussion on the dynamic resistance data.

For the MgO barrier, R_D shows valleys at $\theta = 90°$, $270°$ at low bias, which are seen as dark areas in Fig. 3(a). The emergence of a second set of peaks can be clearly distinguished above a threshold voltage of ~ -0.4 V and $+0.45$ V, for negative and positive voltages, respectively.
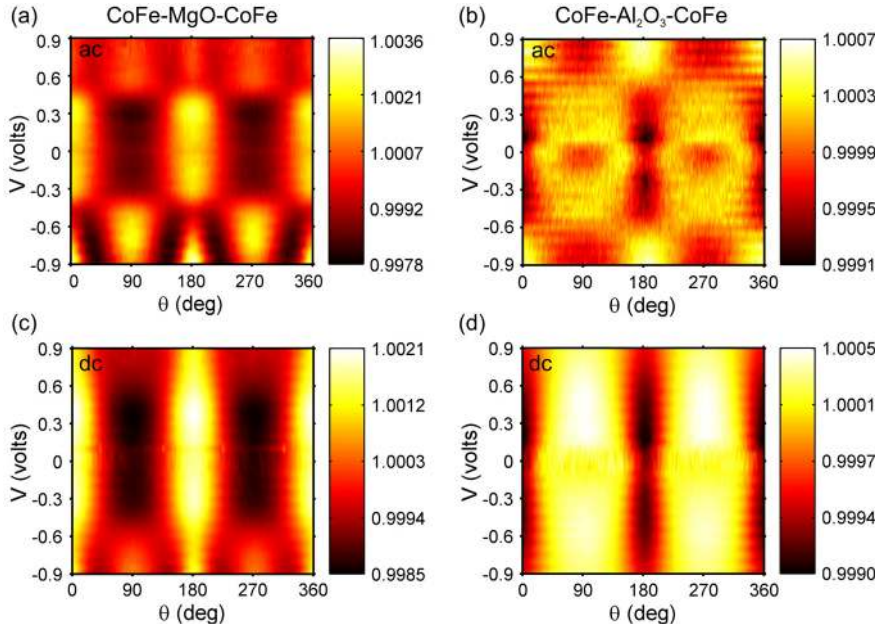
FIG. 3 (color online). (a),(b) Contour plots of R_D as a function of bias and angle for the MgO and Al_2O_3 MTJs. (c),(d) The corresponding contour plots of dc resistance.

Note that this distinctive change in the angular dependence is obscured in the dc resistance plot. Above this threshold voltage the angular dependence shows clear evidence for some fourfold character.

The TAMR effect of the Al_2O_3 junction has distinctly different characteristics compared with that of the MgO junction, as shown in Figs. 2(b), 3(b), and 3(d). Generally speaking, the TAMR magnitude is much smaller than that of the MgO junction. In the low bias regime, the R_D vs θ curve contains a fourfold symmetric component with minima at $\theta = 0°$ and $90°$. As the bias increases, the curve becomes largely twofold symmetric. Below $\sim \pm 0.6$ V, the curve has a maximum at $\theta = 90°$ and a minimum at $\theta = 0°$. Above $\sim \pm 0.6$ V, however, the positions for the resistance extrema are reversed; i.e., the maximum is at $\theta = 0°$ and the minimum is at $\theta = 90°$. These features are clearly seen in Fig. 3(b). Note that the basic characteristics of the contour plots shown in Fig. 3 do not change with field for the field range explored (from 5 to 9 T).

To check that the observed TAMR results from spin-dependent tunneling, we fabricated tunnel junctions with nonmagnetic aluminum electrodes with the following structure: 100 MgO/150 Al/32 MgO/150 Al/100 Ta (layer thicknesses in Å). No TAMR was measured within the experimental noise level for these control samples.

The R_D vs θ curve at a given bias can be fitted using the following equations:

$$R_D(\theta) = (A_0 + A_2 \cos 2\phi + A_4 \cos 4\phi)^{-1}, \qquad (1)$$

$$\frac{\cos\phi}{\sin\phi} = \frac{H\cos\theta - 4\pi M_s \cos\phi}{H \sin\theta}, \qquad (2)$$

where ϕ is the angle between the CoFe magnetization direction and the film normal direction $\vec{n}$ after taking into account the demagnetization field; M_s is the saturation

magnetization of CoFe; A_0, A_2, and A_4 are fitting parameters. The ratios A_2/A_0 and A_4/A_0 can be understood as half of the TAMR magnitude of the components with twofold and fourfold symmetries, respectively. Their signs are related to the positions of the resistance extrema in the R_D vs θ curves. Assuming $4\pi M_S = 1.93$ T, excellent agreement between data and fits are obtained [see Figs. 2(a) and 2(b)]. A_2/A_0 and A_4/A_0 values, obtained from the fits, are plotted in Figs. 2(c) and 2(d), which show very complicated bias dependences for both types of junctions.

The TAMR effect likely originates from SOC, which gives rise to an anisotropy of the DOS of the bulk electrodes [9,10,12] and that of their interfaces [13] with respect to the magnetization direction. The pronounced difference between the MgO and Al_2O_3 MTJs points to the interface electronic structure as the origin of the TAMR.

Using a simple tight-binding model, we demonstrate that the influence of resonant states on the interface DOS of the majority band can lead to the observed evolution of TAMR from a twofold to a fourfold angular dependence. Note that we have examined the band structure of bcc CoFe along the $\Gamma - H$ ($k_{||} = 0$) direction in the Brillouin zone. Specifically, we explored the lifting of degeneracy in the bulk band structure due to SOC and found no fourfold component in the angular dependence of the DOS at any energy sufficient to lead to the observed variation in the experiments. This suggests that the fourfold component does not arise from the bulk band structure of CoFe.

We model the Δ_1 majority-spin band in bcc CoFe [4] by a one-dimensional tight-binding band. We consider the case when this band is coupled to a minority resonant state localized at the interface via SOC described by the parameter λ. The anisotropy in the conductance is determined by the anisotropy of the interface DOS of the majority Δ_1 band, which can be found from the corre-
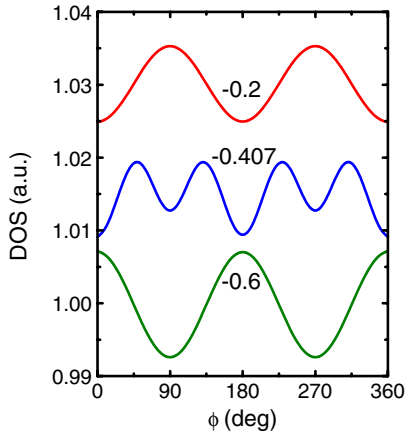
FIG. 4 (color online).   Angular dependence of the interface
DOS of the majority band (in arbitrary units) for several energies
E near the resonant energy $E_r = -0.4$ eV. Energies are given in
eV. The majority band has width 4 eV and is centered at 0.6 eV.
The width of the resonant state $\gamma_0 = 10$ meV, and the spin-orbit
coupling parameter $\lambda = 50$ meV.

sponding interface Green's function, $g(E)$. We note that,
due to the weak energy dependence of the Δ_1 electron
band's decay function through a crystalline MgO barrier
[4], states far below E_F can significantly contribute to the
tunneling current, contrary to the free electron band case
[14]. By solving Dyson's equation we find that

$$g(E) = \frac{g_0(E)}{1 - \lambda^2 g_0(E) g_r(E) \cos^2 \phi}, \qquad (3)$$

where $g_0(E)$ is the interface Green's function of the ma-
jority band in the absence of SOC [15] and $g_r(E) = (E -
E_r + i\gamma_0)^{-1}$ is the Green's function of the resonant level
with E_r and γ_0 being the resonance energy and width,
respectively.

In Fig. 4 we plot the interface DOS of the majority band,
$\rho = -\mathrm{Im}(g)/\pi$, as a function of ϕ for several energies
near the resonant level which we have chosen to lie at $E_r =
-0.4$ eV. Away from the resonance the angular depen-
dence of the interface DOS has a twofold symmetry. This
twofold angular dependence changes sign near the reso-
nant energy. Associated with this sign change is the onset
of a significant fourfold angular variation. Since the tun-
neling current will largely be determined by the interface
DOS of the majority Δ_1 channel, this same variation will
appear in the R_D measurement when the window of applied
bias passes the resonance.

It is known that the bcc Fe(001) surface supports a
minority-spin surface state [16]. The relevant interface
state is present in Fe(001)/MgO/Fe tunnel junctions, as
indicated by theory [4,15] and experiment [17]. A similar
resonant state is likely present at the bcc CoFe(001) surface
and the CoFe(001)/MgO interface. Using a rigid band
model to estimate the change in the Fermi energy due to
the increase in valence of CoFe as compared to Fe, we find

the position of the interface resonant state for
$Co_{70}Fe_{30}(001)/MgO$ interface is ~0.4 eV below the
Fermi energy. This is consistent with the observation of
significant fourfold symmetry for bias beyond ~ −0.4 V
or +0.45 V for MgO based MTJs, as shown in Fig. 2.

In the case of Al_2O_3 based MTJs a similar effect may
occur due to the possibility of a narrow majority interface
resonant band derived from excess oxygen at the interface
[15]. It is predicted that this band lies close to the Fermi
level and is strongly transmitting. An analysis based on a
model similar to that above reveals that an interface reso-
nant DOS also has a significant fourfold angular variation
when coupled to a bulk band via SOC. This is consistent
with the observation of a strong fourfold dependence of the
variation observed in Al_2O_3 at low bias in Fig. 2.

In conclusion, we have observed a tunneling anisotropic
magnetoresistance effect in magnetic tunnel junctions with
$3d$ transition metal ferromagnetic electrodes for both crys-
talline and amorphous tunnel barriers, despite the weak
spin-orbit coupling in these systems. We find complex
dependences of the junction resistance on the bias voltage
and angle, which are distinctly different for MgO and
Al_2O_3 tunnel barriers. A tight-binding model suggests
that the TAMR effect derives from the anisotropy in the
interface density of states of the majority band due to
mixing with a resonant state via spin-orbit coupling.

[1] S. S. P. Parkin *et al.*, Proc. IEEE **91**, 661 (2003).
[2] E. Y. Tsymbal and D. G. Pettifor, J. Phys. Condens. Matter
      9, L411 (1997).
[3] C. Kaiser *et al.*, Phys. Rev. Lett. **94**, 247203 (2005).
[4] W. H. Butler *et al.*, Phys. Rev. B **63**, 054416 (2001).
[5] S. S. P. Parkin *et al.*, Nature Mater. **3**, 862 (2004).
[6] S. Yuasa *et al.*, Nature Mater. **3**, 868 (2004).
[7] J. J. Yang *et al.*, Appl. Phys. Lett. **89**, 202502 (2006).
[8] J. Hayakawa *et al.*, Appl. Phys. Lett. **89**, 232510 (2006).
[9] C. Gould *et al.*, Phys. Rev. Lett. **93**, 117203 (2004).
[10] C. Rüster *et al.*, Phys. Rev. Lett. **94**, 027203 (2005).
[11] H. Saito, S. Yuasa, and K. Ando, Phys. Rev. Lett. **95**,
      086604 (2005).
[12] A. B. Shick *et al.*, Phys. Rev. B **73**, 024418 (2006).
[13] A. N. Chantis *et al.*, Phys. Rev. Lett. **98**, 046601 (2007).
[14] The weak energy dependence of the electron's decay
      function is due not only to the particular band structure
      of MgO but also to the Fermi level lying near the band gap
      center. If the Fermi level were close to either the conduc-
      tion or the valence band, the variation of the decay
      constant with energy could not be ignored.
[15] E. Y. Tsymbal *et al.*, Prog. Mater. Sci. **52**, 401 (2007).
[16] J. A. Stroscio *et al.*, Phys. Rev. Lett. **75**, 2960 (1995).
[17] C. Tiusan *et al.*, Phys. Rev. Lett. **93**, 106602 (2004).